

Ozone Photochemistry and the Role of PAN in the Springtime Northeastern Pacific

Troposphere: Results from the PHOBEA Campaign

Robert A. Kotchenruther¹, Daniel A. Jaffe^{2,3}, and Lyatt Jaeglé³

¹University of Washington Seattle, Department of Chemistry

²University of Washington Bothell, Interdisciplinary Arts and Sciences

³University of Washington Seattle, Department of Atmospheric Sciences

Kotchenruther, R. A., D. A. Jaffe, and L. Jaeglé, Ozone photochemistry and the role of PAN in the springtime Northeastern Pacific Troposphere: Results from the PHOBEA campaign, *J. Geophys. Res.*, 106, 28,731-28,741, 2001.

Abstract:

In the spring of 1999 airborne measurements of NO, O₃, PAN, CO, CH₄, H₂O, volatile organic compounds, aerosols (particle count, light scattering, and light absorption), NO₂ photolysis frequency, and standard meteorological variables were made off the coast of Washington State as part of the Photochemical Ozone Budget of the Eastern North Pacific Atmosphere (PHOBEA) experiment. These measurements were used to constrain a photochemical box model to calculate the ozone photochemical tendency, T(O₃), in this region. T(O₃) in marine flow from the remote Pacific was found to be weakly ozone destroying from the surface up to 8 km. Values of T(O₃) increased from -0.83 ppbv/day in the 0-2 km layer to -0.11 ppbv/day in the 6-8 km layer. These results are compared to T(O₃) from other photochemistry experiments in the springtime Pacific. We also used the model to investigate the impacts of PAN decomposition on the mixing ratio of NO_x (defined here as NO+NO₂+NO₃+2N₂O₅+HNO₂+HNO₄) and on T(O₃). PAN decomposition was found to contribute from 11 to 30% towards NO_x production and to enhance T(O₃) by 0.13 to 0.41 ppbv/day. The impacts of PAN decomposition were further investigated in a case study where measurements were made in a strongly subsiding air mass. In this air mass, PAN induced perturbations to NO_x and T(O₃) reached 20.1 pptv and 1.45 ppbv/day, respectively, more than three times that found in marine background average. Finally we estimate how T(O₃) in the Northeast Pacific atmosphere may change as a result of increasing anthropogenic NO_x emissions from Asia. The calculations suggest that while O₃ mixing ratios in the Northeast Pacific are likely to increase, T(O₃) will remain close to its current value as a result of offsetting factors.

1. Introduction

Tropospheric ozone plays an important role in a number of atmospheric phenomena. Ozone is the chief source of hydroxyl radical (OH), the primary oxidant of trace gases in the troposphere (Levy 1971; Crutzen et al., 1999 and references therein). Because oxidation is the main removal pathway for many trace gases, ozone plays an indirect but crucial role in determining both the oxidative potential of the atmosphere, and the lifetime of many trace gases. Tropospheric ozone is a pollutant which has been shown to have adverse effects on plant life even at current background levels (Guderian et al., 1985). Anthropogenic increases in tropospheric ozone also contribute to radiative forcing of the atmosphere (Lacis et al., 1990; IPCC, 1996).

Measurements (Bojkov, 1986; Volz and Kley, 1988; Guicherit and Roemer, 2000) and modeling (Wang and Jacob, 1998; McKeen et al., 1989) of ozone mixing ratios in the troposphere have shown an increasing trend throughout the 20th Century. East Asia, in particular, is a region currently experiencing rapid economic growth and increasing emissions of trace gases associated with ozone production (Akimoto and Narita, 1994; Elliott et al., 1997; VanArdeen et al., 1999; Streets and Waldhoff, 2000). As a result, ozone in the boundary layer and lower troposphere of this region has been increasing by about 2% per year (Logan, 1994; Lee et al., 1998). Because ozone has a long lifetime (~ months), it is likely that this positive trend in ozone impacts regions down wind of the Asian continent (Mauzerall et al., 2000). Global modeling studies by Berntsen et al. (1999) and Jacob et al. (1999) have predicted an increase of roughly 4 ppbv in surface ozone over Western North America due to a doubling of Asian emissions.

Because NO_x has a short lifetime in the lower troposphere (~ 1 day), the transport of longer lived NO_x reservoirs such as PAN and HNO₃ can play an important role in perturbing ozone photochemistry in regions

remote from direct NO_x emissions (Singh et al., 1992; Yienger et al., 1999). Moxim et al. (1996) and Horowitz and Jacob (1999) have found PAN to be the most significant NO_x reservoir with respect to northern mid-latitude springtime ozone photochemistry. During winter months in northern high latitudes PAN's concentration increases due to PAN's long lifetime at cold temperatures. Springtime warming events lead to high rates of PAN thermal decomposition, releasing the stored NO₂ (Beine et al., 1997; Herring et al., 1997). Measurements at Mauna Loa Hawaii (Hauglustaine et al., 1996) and modeling efforts (Moxim et al., 1996) suggest that NO_x levels over the remote Pacific Ocean are near the balance point between ozone photochemical production and destruction. A number of recent ground based studies have shown that PAN thermal decomposition can influence ozone concentrations regionally (Beine et al., 1997) and that this influence can be significant in remote areas (Hov et al., 1997). Global models have also been employed to estimate the distribution of PAN in the North Pacific troposphere (Thakur et al., 1999) as well as estimate PAN's impact on NO_x concentrations (Moxim et al., 1996; Horowitz and Jacob, 1999). In their modeling work, Moxim et al. estimated that PAN thermal decomposition can increase NO_x concentrations in the remote lower troposphere by up to a factor of five during spring. Horowitz and Jacob estimated that 80% of the NO_x having fossil fuel combustion as its source is transported into the Northeastern Pacific troposphere as PAN.

In this study we analyze springtime aircraft measurements of trace gases involved in ozone photochemistry, which were gathered in 1999 off the coast of Washington State. These measurements were part of the Photochemical Ozone Budget of the Eastern North Pacific Atmosphere (PHOBEA) experiment. The PHOBEA experiment included both ground-based measurements at the Cheeka Peak Observatory on the coast of Washington State (Jaffe et al., 1999; Jaffe et al., 2001) and airborne measurements using the University of Wyoming's King Air research aircraft (Kotchenruther et al., 2001). The primary goals of the PHOBEA experiment were to quantify the ozone photochemical tendency over the remote Northeastern Pacific ocean, investigate the impacts of PAN decomposition on NO_x and ozone photochemistry, and investigate the impacts of long range transport of anthropogenic emissions from the Northwestern Pacific on the chemical composition of air over the Northeastern Pacific Ocean. In this study we employ a detailed photochemical box model constrained by the PHOBEA aircraft data to calculate the ozone photochemical tendency in the springtime Northeastern Pacific troposphere and to explore its controlling factors.

2. Experimental

2.1 Measurements

From March 26 to April 28 of 1999 the University of Wyoming's King Air 200T research aircraft made 14 flights over the Northeastern Pacific Ocean between 39-48°N latitude, 125-129°W longitude, and at altitudes between 0-8 km. A detailed description and analysis of measurements and meteorological conditions during the aircraft portion of the PHOBEA experiment can be found in Kotchenruther et al. (2001). Therefore, here we give only a brief description.

The aircraft was equipped with instrumentation to measure NO, O₃, PAN, CO, CH₄, H₂O, volatile organic compounds (VOCs), aerosols (number density, light scattering, and light absorption), NO₂ photolysis frequency, J(NO₂), and standard meteorological variables. Flights were scheduled to maximize the amount of time spent in the experiment area during high sun conditions. Local noon was at approximately 12:30 p.m. (PST). Sampling during each flight was done over the Pacific Ocean in 6 to 10 level flight legs of 20 minute duration. The only exception to this standard sampling pattern was on April 21 (flight 11), where the aircraft flew south down the coast of Oregon and into Northern California making measurements at only two altitudes. This flight was used to investigate the impacts of PAN decomposition in a strongly subsiding air mass, which was centered off the coast of Northern California.

Operational forecasting for research flights was conducted with the goal of sampling air that had not recently (within 3 days) been exposed to continental influence. The measured air masses were overwhelmingly from the remote Pacific, 5-20 days from the Eurasian continent.

2.2 Modeling

These trace gas and aerosol measurements are used to constrain a photochemical 0-D model. The model is essentially identical to that presented in Jaeglé et al. (2000) and Schultz et al. (2000). We used this model to calculate the ozone photochemical tendency and investigate NO_x chemistry in the low to mid troposphere over the Northeastern Pacific Ocean.

Model calculations were constrained by the measured mixing ratios of NO, O₃, PAN, CO, CH₄, H₂O, and VOCs, temperature, pressure, latitude and longitude of the measurement location (Table 1). The concentration of NO_x (= NO + NO₂ + NO₃ + 2 N₂O₅ + HNO₄) is calculated in the model such that the calculated NO matches the observed NO at the time of day of observations.

Ozone column concentrations were obtained from TOMS satellite observations (from the NASA web site <http://jwocky.gsfc.nasa.gov/>) and ranged between 304 and 413 Dobson units (DU) throughout the aircraft campaign, the average for the campaign was 363 DU. The model uses a radiative transfer code to calculate

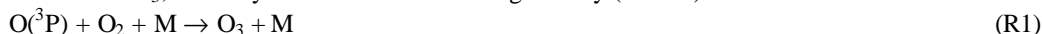
photolysis rates based on clear sky conditions. However, the presence of clouds caused significant deviations between the model calculated clear sky $J(\text{NO}_2)$, and measured $J(\text{NO}_2)$. To account for these effects, we multiplied all model calculated clear-sky photolysis rates by a scaling factor defined by the ratio $J(\text{NO}_2)_{\text{measured}}/J(\text{NO}_2)_{\text{clear sky}}$ [Jaeglé et al., 2000]. This ratio ranged from 1.1 in the 0-2 km layer to 1.4 in the 6-8 km layer.

Aerosol surface area was estimated from the wavelength dependence of aerosol light scattering and calculations based on Mie theory, yielding surface areas between 2.5 and 5.5 $\mu\text{m}^2/\text{cm}^3$.

With its long photochemical lifetime (~1 month), it is likely that HNO_3 is not in diel steady state. Because HNO_3 plays a significant role in the budget of NO_x in the remote troposphere, we decided to constrain the model with the average springtime vertical profile of HNO_3 compiled by Thakur et al. [1999] for the Northeastern Pacific. This is a reasonable assumption as our measured concentration profiles of PAN and NO are in good agreement with the Northeastern Pacific averages reported by Thakur et al. [1999]. In addition we constrained the concentrations of peroxypropionyl nitrate (PPN) by defining the ratio of PPN/PAN to be 0.09, which is the average from previous springtime measurements in the Northeastern Pacific (Singh and Salas, 1989).

2.3 Calculation of the ozone photochemical tendency

Assuming that cycling between NO_2 and NO only occurs through the photolysis of NO_2 and the reaction of NO with O_3 , a null cycle is established during the day (R1-R3).



However, the presence of peroxy radicals provides an alternate pathway that converts NO to NO_2 without consuming ozone (R4-R6), leading to net ozone production.



In R6, RO_2 refers to peroxy radicals from C2 and larger hydrocarbons. The rate of ozone production, $\text{P}(\text{O}_3)$, can then be expressed as:

$$\text{P}(\text{O}_3) = \{ k_4[\text{HO}_2] + k_5[\text{CH}_3\text{O}_2] + k_6[\text{RO}_2] \} [\text{NO}] \quad (1)$$

where $[\text{HO}_2]$, $[\text{CH}_3\text{O}_2]$, $[\text{RO}_2]$, and $[\text{NO}]$ are the concentrations of HO_2 , CH_3O_2 , RO_2 , and NO in molecules cm^{-3} , respectively, and k_4 , k_5 , and k_6 the rate constants of reactions R4, R5, and R6 in molecules⁻¹ $\text{cm}^3 \text{s}^{-1}$, respectively (Crawford et al., 1997a).

Ozone loss in the remote troposphere occurs primarily through photolysis and the reactions with OH and HO_2 (R7-R10).



The rate of ozone loss, $\text{L}(\text{O}_3)$, can then be expressed as:

$$\text{L}(\text{O}_3) = k_8[\text{O}(^1\text{D})][\text{H}_2\text{O}] + k_9[\text{OH}][\text{O}_3] + k_{10}[\text{HO}_2][\text{O}_3] \quad (2)$$

Hence, the net ozone photochemical tendency, $\text{T}(\text{O}_3)$, can be expressed as (Crawford et al., 1997a; Crutzen et al., 1999):

$$\text{T}(\text{O}_3) = \text{P}(\text{O}_3) - \text{L}(\text{O}_3) \quad (3)$$

3. Results

3.1 Ozone photochemical tendency in the remote Northeastern Pacific troposphere

The PHOBEA aircraft measurements were averaged into 2 km bins from 0-8 km and the model runs were based on these average values. Table 1 presents the averages used to constrain the model. Model results were also calculated based on the data from individual 20-minute flight segments. However, running the model using each flight segment was problematic because hydrocarbon data were only available for about half the flight segments. The average $\text{T}(\text{O}_3)$ values calculated by these two different approaches were within 0.2 ppbv/day at all altitudes. In the remainder of this paper model calculated values are based on the 2 km averages, except as noted below for the case study in section 3.4. Model calculated mixing ratios of NO_x , NO_2 , HNO_4 , OH, HO_2 , and CH_3O_2 are presented in Table 2. In addition, Table 2 also presents the production and loss rates of NO_x and O_3 , and the resulting $\text{T}(\text{O}_3)$. Unless otherwise noted, all rates and the quantities derived from rates are the steady state values averaged over a 24 hour diel cycle, whereas all mixing ratios are those measured at, or calculated for, the time of measurement (within two hours of solar noon).

The model calculations (Table 2) show an imbalance between known NO_x sources and sinks at all

altitudes: the NO_x loss rate exceeds its production. Imbalances of this kind have also been found in numerous other experiments (Hauglustaine et al., 1999 and references therein). Our calculations suggest that additional sources of NO_x ranging from 27-29 pptv/day in the layers from 0-6 km and 6 pptv/day in the 6-8 km layer are required to establish balance. Most authors have attributed imbalances to unspecified reactions that recycle HNO₃ back to NO_x and have proposed several heterogeneous and homogeneous reactions to account for this (Hauglustaine et al., 1999). However, direct emissions of NO_x from shipping and aircraft can be sources of imbalance, and our assumptions about HNO₃ and PPN mixing ratios create large uncertainties in the rate of NO_x production.

The NO_x lifetimes listed in Table 2 (defined as the inverse loss frequency, the NO_x burden divided by the NO_x loss rate), of less than a day near the boundary layer and several days in the mid troposphere, are consistent with previous studies (Brasseur et al., 1999).

The calculated T(O₃) for the remote springtime Northeastern Pacific is weakly ozone destroying, with values increasing from -0.83 ppbv/day in the 0-2 km layer to -0.11 ppbv/day in the 6-8 km layer.

Figure 1 depicts model estimated P(O₃) and L(O₃) delineated by reaction as well as the percent contribution by each reaction towards the total. The reaction of HO₂ with NO (R4) plays the dominant role in ozone production, accounting for 65% in the 0-2 km layer and increasing to 77% in the 6-8 km layer. The sum of HO₂ and CH₃O₂ reactions with NO (R4 and R5) make up roughly 90% of ozone production throughout the lower troposphere. Ozone loss is also dominated by HO₂, with the HO₂ + O₃ reaction (R10) accounting for 47% of ozone loss in the 0-2 km layer and increasing to 64% in the 6-8 km layer. This is typical for high latitudes where J(O₃) is reduced by larger total ozone columns and solar zenith angles (Herring et al., 1997; Crawford et al., 1997b). Ozone photolysis and the resulting O(¹D) reaction with H₂O also plays an important role in ozone loss near the surface, accounting for 44% of L(O₃), but this influence decreases to 21% in the 6-8 km layer due to the rapid decline in water vapor concentration with increasing altitude.

Figure 2 compares T(O₃) in the remote Northeastern Pacific during PHOBEA with other springtime photochemistry experiments in the Pacific basin. Two other experiments are considered here; PEM West B and MLOPEX 2. PEM West B took place during February – March 1994 in the Western Pacific where air masses were segregated into three categories; flow from the remote tropical Pacific (Crawford et al., 1997a), Asian continental outflow between 20-30°N latitude (Crawford et al., 1997b), and Asian continental outflow between 30-50°N latitude (Crawford et al., 1997b). MLOPEX 2 took place in four intensive campaigns throughout 1992 and included springtime measurements from the free troposphere (Hauglustaine et al., 1999). Roughly two thirds of air masses arriving at Mauna Loa Observatory during MLOPEX 2 had a westerly track from the mid-latitude Pacific, with the remainder being easterly from the tropical or sub-tropical Pacific.

Several trends in springtime T(O₃) are suggested in Figure 2. A longitudinal trend across the mid-latitude Pacific, with net ozone production occurring in the Northwestern Pacific transitioning to net ozone destruction in the remote Northeastern Pacific. Net ozone production dominates the mid-latitude Northwestern Pacific due to the influence of anthropogenic emissions in the Asian continental outflow. However, because of the short lifetime of NO_x in the troposphere (~ 1 day) and an average transport time across the Pacific of 8-10 days (Kotchenruther et al., 2001), NO_x mixing ratios become very low in the Eastern Pacific, resulting in net ozone destruction. A latitudinal trend in the remote Pacific is also suggested in Figure 2, where higher rates of ozone destruction occur in the remote tropical Pacific and weaker ozone destruction as one moves northward. This trend is the result of a number of factors. As one moves from the tropical Pacific to the mid-latitudes; actinic flux diminishes, water vapor concentrations diminish, PAN concentrations increase, and the NO_x lifetime increases. These factors outweigh the influence of higher ozone loss rates caused by increasing ozone concentrations at higher latitudes.

T(O₃) from the CITE 1 experiment (Chameides et al., 1989) in the Northeastern Pacific is not reported in Figure 2 for several reasons. Chameides et al. only report T(O₃) at the time of measurement, rather than a 24 hour average, and the origin of measured air masses was not well established (e.g., continental vs. remote marine). Having said that, we can compare T(O₃) during CITE 1 and PHOBEA at the time of measurement. Chameides et al. report values of T(O₃) between -38×10^5 and -50×10^5 molecules cm⁻³ s⁻¹ for the 0-2 km layer in the Northeastern Pacific near solar noon, and they found that T(O₃) increased to near zero in the 6-8 km layer. By comparison, during PHOBEA T(O₃) was -8.1×10^5 molecules cm⁻³ s⁻¹ near solar noon for the 0-2 km layer, increasing to near zero in the 6-8 km layer. The differences in T(O₃) likely reflect the dissimilarity in the latitude ranges of measurement, 24-40°N latitude and 39-48°N latitude for CITE 1 and PHOBEA, respectively, and the dissimilarity in time of year, early May and late March – April for CITE 1 and PHOBEA, respectively.

3.2 Impacts of PAN decomposition and ship exhaust plumes on NO_x and T(O₃)

Table 2 lists the PAN loss rate, which we define here as the sum of the reaction rates for thermal decomposition (R11) and photolysis (R12) after correcting for cycling within the PAN_x (=PAN+CH₃CO₃) family (Jacob et al., 1996).



PAN thermal decomposition accounted for 96, 72, 19, and 2% of the total PAN loss rate in the 0-2, 2-4, 4-6, and 6-8 km layers, respectively. PAN's fractional contribution to NO_x, listed in Table 2, was calculated as the ratio of the PAN loss rate to NO_x loss rate, rather than the ratio of PAN loss rate to NO_x production rate. Essentially, by making the calculation with the NO_x loss rate, we assume that NO_x production and loss are in balance and that the imbalances reported in Table 2 reflect both the uncertainty in NO_x production and loss rates, and possible missing sources of NO_x. As discussed above, the NO_x production rates have a higher uncertainty compared to loss rates because they are largely dependent on the mixing ratios of HNO₃, PAN, and PPN, of which HNO₃ and PPN were prescribed in the model but not measured during PHOBEA. However, the NO_x loss rate depends primarily on the conversion of NO₂ to HNO₃, PAN, and PPN. Because NO₂ is calculated from NO and J(NO₂) measurements, it is likely that NO_x loss rates have less uncertainty. With these assumptions, we find that PAN's contribution to NO_x decreased from 30% in the 0-2 km layer to 11% in the 4-6 km layer and then increased to 18% in the 6-8 km layer. The increase in the 6-8 km layer is primarily due to the increasing lifetime of NO_x in that layer, 3.2 days, as compared to 1.1 days in the 4-6 km layer, and is only weakly associated with increased photolysis.

We also estimated the impact of PAN decomposition on P(O₃) using equation (4):

$$\Delta\text{P}(\text{O}_3)_{\text{PAN}} = \frac{(\text{PAN Loss Rate})}{(\text{NO}_x \text{ Loss Rate})} \text{P}(\text{O}_3) \quad (4)$$

Equation (4) calculates PAN's effect on P(O₃) by scaling the NO concentration in P(O₃) to the amount caused by PAN decomposition. Therefore, ΔP(O₃)_{PAN} can be considered the perturbation to P(O₃) caused by PAN decomposition. It should be noted that PAN decomposition had little effect on L(O₃) (Klonecki and Levy, 1997), hence, ΔP(O₃)_{PAN} can also be viewed as the perturbation to T(O₃) caused by PAN decomposition. Figure 3 depicts the sum of NO+NO₂ and T(O₃), both including and excluding the effects of PAN decomposition. The ratio of the observed NO+NO₂ to NO+NO₂ without PAN decomposition ranged from 1.4 in the 0-2 km layer, decreasing to 1.1 in the 4-6 km layer. This is within the range of values of this ratio computed from a global modeling study by Moxim et al. (1996). The values of this ratio calculated by Moxim et al. were from 1-5 for this region of the Pacific in January and from 1-2 in July. Table 2 shows that PAN decomposition increases P(O₃) from 11 – 30%, bringing T(O₃) closer to the balance point between ozone production and destruction (figure 3b), and thus induces a significant perturbation to ozone photochemistry in this region.

Ship exhaust plumes were identified only in the 0-2 km layer during PHOBEA. When the NO data from ship plumes was included with the rest of the data, the mean NO mixing ratio increased from 9.5 to 12.6 pptv and a value of 41.4 pptv for NO_x was then required in the model. This resulted in -0.46 ppbv/day for T(O₃), that is, an enhancement in of +0.37 ppbv/day over the background without ship plumes. It must be said, however, that adding NO data from very fresh ship plumes, to the marine background, is not likely to give an accurate estimate of shipping's general influence on the marine boundary layer. The frequency with which we encountered ship exhaust plumes may not be representative of the average, and accounting for ship plume influence by this method is a simplistic approach that assumes plumes diffuse into the background without photochemical removal, which is inaccurate because the time for plume diffusion is likely on the order of the lifetime of NO_x.

3.3 The impact of doubled Asian emissions on T(O₃) in the springtime Northeastern Pacific and the sensitivity of T(O₃) to enhancements in NO_x, CO, and O₃.

The remote marine troposphere, and in particular the remote Pacific troposphere has been found here, and during previous experiments, to be under a regime of net ozone destruction. Consequently, remote marine environments can be considered buffers against anthropogenic increases in global tropospheric ozone (Brasseur et al., 1999). Because the Pacific Ocean occupies approximately one third of the earth's surface, it therefore provides one of the largest buffers against global increases in tropospheric ozone. However, recent rapid industrialization in eastern Asia and the subsequent enhancements in ozone producing trace gases may be significantly eroding the buffering potential of the remote Pacific. Indeed, Crawford et al. (1997b) found enhanced NO_x and net ozone production in air masses impacted by Asian emissions that were advected ~2000 km east of the Asian continent.

Previously Bernsten et al. [1999] used a global chemical transport model to estimate the effects of doubling Asian anthropogenic emissions, based on 1996 emission levels, on the mixing ratios of NO_x, PAN, CO, and O₃ in the springtime *Northeastern* Pacific. They present results for the model grid just west of Cheeka Park Observatory, over the Pacific Ocean. This also corresponds to the experiment area during PHOBEA's

airborne measurements. When Asian anthropogenic emissions were doubled they found that NO_x, PAN, CO, and O₃ were enhanced in the Northeastern Pacific by 16-24%, 30-40%, 25-26% and 7-10%, respectively, throughout the tropospheric column. Generally, the largest enhancements for all species were in the lower free troposphere (Berntsen, personal communication, 2000). In this study, we used the 0-D model to explore how these changes impact T(O₃) in the Northeastern Pacific. To do this we increased the constrained values of NO_x, PAN, CO, and O₃ by the appropriate amount in each altitude bin and calculated T(O₃) under these new conditions.

Figure 4a depicts T(O₃) in the remote marine background and T(O₃) incorporating enhancements in NO_x, PAN, CO, and O₃ based on doubled Asian emissions. While T(O₃) remained essentially unchanged under the scenario of doubled Asian emissions, the rates of P(O₃) and L(O₃) were significantly increased; P(O₃) increased from 9-21% and L(O₃) increased from 13-16%.

In order to understand the impact of each species on P(O₃), L(O₃), and T(O₃), we conducted a series of sensitivity studies where model constraints were held constant and one species was sequentially increased. In the sensitivity studies, the concentrations of NO_x and O₃ were each increased by 10, 20, 30, 40, and 50%, and CO was increased by 25, 50, 75, and 100% over their original, measured, mixing ratios. The sensitivity of T(O₃), P(O₃) and L(O₃) to these increases is depicted in Figures 4b-d and 5.

Increasing NO_x results in increasing P(O₃) (equations (1) and (3)) with little effect on L(O₃) (equation (2)), yielding an increase in T(O₃). Enhancing PAN in the model had no effect on T(O₃) because NO_x was constrained and held constant. However, enhancing PAN did effect the balance between NO_x production and loss by increasing the NO_x production rate.

Increasing NO_x had the effect of shifting P(O₃), and therefore T(O₃), to more positive values (figures 4b and 5a), as expected from equations (1) and (3). As expected from equation 2, there was little effect on L(O₃).

Higher CO mixing ratios had a small effect, shifting T(O₃) to more negative values. Reaction with CO is the main pathway for converting OH to HO₂ radicals in the remote troposphere. Equations (1) and (2) and Figure 1 shows that HO₂ plays a role in both ozone production and loss. Whether production or loss is dominant depends on the relative amounts of NO and O₃ present. The increase in L(O₃) resulting from a higher CO concentrations (and thus higher HO₂ levels) outweighs the increase in P(O₃). As a result, T(O₃) decreases with increasing CO (figures 4c, 5c and 5d).

Increasing O₃ had the effect of strongly shifting T(O₃) to more negative values. Increasing O₃ directly leads to larger L(O₃) as shown in equation (2). Additionally, as the main source of OH, and because of rapid cycling between OH and HO₂, increasing O₃ indirectly increases HO₂, which further enhances L(O₃) as discussed for CO above.

These calculations suggest that, while ozone mixing ratios will increase under the scenario of doubled Asian emissions, the ozone photochemical tendency in the Northeastern Pacific will remain close to its current value. This is primarily the result of the offsetting affects of enhanced O₃ and NO_x. The positive shift in T(O₃) from higher NO_x mixing ratios balances the decrease in T(O₃) from enhanced O₃ and CO.

3.4 The effects of PAN decomposition on NO_x and T(O₃) in a strongly subsiding air mass.

A frequent synoptic scale feature of the springtime Northeastern Pacific is a broad region of high sea level pressure climatologically centered at 140°W longitude and 35°N latitude. The position of this high pressure center typically generates strong subsidence in air masses above Northern California during the spring. On April 21, 1999 the high pressure center off the coast reached 1030 mb, roughly 5 mb higher than the average. At this time, the strongest levels of subsidence were centered at 122°W longitude and 36°N latitude, with a peak subsidence rate of 15 mb/hr at 500 mb. On this date we conducted PHOBEA flight 11, making measurements of trace gases and aerosols while flying into this region of strong subsidence. The flight was conducted such that measurements in the experiment area were centered at solar noon. The aircraft first flew south at an altitude of 1.5 km along a line of constant longitude (124.80°W), which was over the Pacific Ocean off the coast of Southern Oregon and Northern California. Due to fuel limitations, after reaching 39.5°N latitude the aircraft ascended to 3.0 km and returned north along the same longitude line. Figure 6a depicts this portion of the aircraft flight track and Figures 6b and 6c depict atmospheric soundings from Oakland, California and Medford, Oregon, respectively. The aircraft data during this flight were averaged into seven 20 minute flight segments, three of which were in the south bound leg and four in the north bound leg (see figure 6a). Local winds during the flight ranged from westerly to northwesterly and 5 day back isentropic trajectories indicated that the encountered air masses had not been exposed to the North American continent within that timeframe (Figure 7a).

Back isentropic trajectories were calculated for each flight segment based on the segment midpoint and closest hour. Trajectories were obtained from NOAA's Air Resources Laboratory using HYSPLIT4 (HYbrid Single-Particle Lagrangian Integrated Trajectory Model, 1997, <http://www.arl.noaa.gov/ready/hysplit4.html>) with the NCEP FNL meteorological dataset. Figure 7 depicts the latitude-longitude and altitude-age profiles of the 5 day back isentropic trajectories for each flight segment, and Table 3 lists averages for selected measured

and model calculated quantities.

Atmospheric temperature and dew point soundings from 5 a.m. (local time) that morning showed the presence of a strong subsidence inversion over Oakland California (figure 6b) and the absence of this inversion further north in Medford Oregon (figure 6c). Temperature, dew point temperature, and trajectory data for the flight segments indicate that the aircraft flew in the boundary layer below the subsidence inversion during the southbound leg and above the boundary layer during the northbound leg. Back trajectories from above the boundary layer show that air masses encountered during flight segments 4 and 5 underwent stronger subsidence than those in segments 6 and 7. The PAN and ozone data presented in Table 3 are consistent with this analysis. PAN and ozone mixing ratios during segments 4 and 5 are in good agreement with average measured mixing ratios of PAN and ozone from higher in the troposphere (Table 1).

PAN mixing ratios during flight segments 1-3 in the boundary layer were below the detection limit of the instrument and are reported in Table 3 as half the value of the detection limit. Back trajectories for flight segments 1-3 indicate that the air masses underwent strong subsidence from the mid troposphere 5 days prior to measurement. However, because the air masses resided in the warm boundary layer for 2-3 days prior to being encountered by the aircraft, high rates of thermal decomposition as a sink for PAN was the likely cause for the low PAN mixing ratios.

Table 3 presents PAN's fractional contribution to NO_x along each segment as well as the enhancement in P(O₃) caused by PAN decomposition. PAN's effects were the largest at the most southerly point above the boundary layer, segment 4, where NO_x mixing ratios were enhanced by 20.1 pptv, to a total of 40.1 pptv, and T(O₃) was enhanced by 1.45 ppbv/day, to a value of -1.78 ppbv/day as a result of PAN decomposition. The enhancements encountered in segment 4 were more than three times the average effects of PAN decomposition at the 2-4 km level (Table 2). The fractional contribution of PAN to NO_x was 0.50 in segment 4 compared to 0.20 in the 2-4 km layer of the marine background. The effects of PAN decomposition were found to diminish as the aircraft headed north out of the region of high subsidence.

The subsidence event on April 21 brought high concentrations of both PAN and ozone to lower altitudes. The data in Table 3 allows us to estimate the ozone photochemical tendency that would be associated with the subsidence event in the absence of PAN, that is, $T(O_3) - \Delta P(O_3)_{PAN}$. Hence, without PAN's perturbation to NO_x, the ozone photochemical tendency in flight segment 4 would have been -3.23 ppbv/day, almost twice the observed rate of net ozone destruction. We can therefore view the role of PAN decomposition during subsidence events as significantly increasing the lifetime of mid-tropospheric ozone at the same time as the subsidence brings that ozone closer to the surface where it has a higher potential to impact the health of flora and fauna.

4. Conclusions

Airborne measurements of NO, O₃, PAN, CO, CH₄, H₂O, VOCs, aerosols, J(NO₂), and standard meteorological variables were made in the remote springtime Northeastern Pacific troposphere as part of the PHOBEA experiment. These measurements were used to constrain a detailed photochemical box model, which calculated the ozone photochemical tendency, T(O₃), in this region. T(O₃) was found to increase from -0.83 ppbv/day in the 0-2 km layer to -0.11 ppbv/day in the 6-8 km layer.

The calculated values of T(O₃) in the Northeastern Pacific were compared to T(O₃) reported during other springtime experiments in the Pacific basin. The comparison suggested two trends in T(O₃); a longitudinal trend driven by decreasing anthropogenic influence where T(O₃) decreases from net ozone production in the mid-latitude Northwestern Pacific transitioning to net ozone destruction in the mid-latitude Northeastern Pacific, and a latitudinal trend driven by changes in solar insolation and water vapor with higher rates of net ozone destruction in the remote tropical Pacific and lower rates of net ozone destruction as one moves northward.

PAN in the marine background was found to account for 30% of NO_x (=NO+NO₂+NO₃+2N₂O₅+HNO₂+HNO₄) sources in the 0-2 km layer and 20, 11, and 18% in the 2-4, 4-6, and 6-8 km layers respectively. The effects of PAN decomposition on T(O₃) were calculated and PAN was found to enhance T(O₃) in the marine background by 0.41, 0.30, 0.13, and 0.15 ppbv/day for the 0-2, 2-4, 4-6, and 6-8 km layers, respectively. However, in a strongly subsiding air mass, PAN's perturbation to NO_x and T(O₃) was found to be over three times the average effect in the marine background.

In 1999, Berntsen et al. used a global chemical transport model to estimate the effects of doubling Asian anthropogenic emissions on the mixing ratios of NO_x, PAN, CO, and O₃ in the springtime Northeastern Pacific. When these enhancements were implemented on the PHOBEA data, and T(O₃) recalculated, we found that while O₃ increased under a scenario of doubled Asian emissions, T(O₃) essentially remained unchanged. Sensitivity studies with the model showed that enhancements in ozone destruction, due to higher ozone concentrations, were nearly balanced by higher rates of ozone production, caused by the increase in NO_x. These results suggest that a doubling of Asian anthropogenic emission, while causing higher ozone concentrations, will not significantly alter the ozone buffering potential of the springtime Northeastern Pacific troposphere.

Acknowledgements:

We would like to thank Terje Berntsen (University of Oslo, Department of Geophysics) for supplying us with a more detailed version of the results reported in Berntsen et al. (1999). We would also like to thank Harald Beine, Tad Anderson, Jan Bottenheim, and the University of Wyoming flight crew and pilot for their indispensable assistance during the PHOBEA campaign. This work was supported by the National Science Foundation grant ATM989627.

References:

- Akimoto H. and H. Narita, Distribution of SO₂, NO_x, and CO₂ Emissions from Fuel Combustion and Industrial Activities in Asia with 1°x1° Resolution. *Atmos. Environ.*, 28, 213-225, 1994.
- Beine, H., D. Jaffe, J. Herring, J. Kelly, T. Krognes, and F. Stordal, High-latitude springtime photochemistry. Part I: NO_x, PAN, and ozone relationships, *J. Atmos. Chem.*, 27, 127-153, 1997.
- Berntsen, T., S. Karlsdottir, and D. Jaffe, Influence of Asian emissions on the composition of air reaching the North Western United States, *Geophys. Res. Lett.*, 26, 2171-2174, 1999.
- Bojkov, R. D., Surface ozone during the second half of the nineteenth century, *J. Am. Meteorol. Soc.*, 25, 343-352, 1986.
- Brasseur, G. P., J. J. Orlando, and G. S. Tyndall (editors), *Atmospheric Chemistry and Global Change*, Oxford University Press, New York, 1999.
- Chameides, W. L., D. D. Davis, G. L. Gregory, G. Sachse, and A. L. Torres. Ozone precursors and ozone photochemistry over eastern North Pacific during the spring of 1984 based on the NASA GTE/CITE 1 airborne observations, *J. Geophys. Res.*, 94, 9799-9808, 1989.
- Crawford J. H., D. D. Davis, G. Chen, J. Bradshaw, S. Sandholm, Y. Kondo, J. Merrill, S. Liu, E. Browell, G. Gregory, B. Anderson, G. Sachse, J. Barrick, D. Blake, R. Talbot, and R. Pueschel, Implications of large scale shifts in tropospheric NO_x levels in the remote tropical Pacific, *J. Geophys. Res.*, 102, 28,447-28,468, 1997a.
- Crawford J., D. Davis, G. Chen, J. Bradshaw, S. Sandholm, Y. Kondo, S. Liu, E. Browell, G. Gregory, B. Anderson, G. Sachse, J. Collins, J. Barrick, D. Blake, R. Talbot, and H. Singh, An assessment of ozone photochemistry in the extratropical western North Pacific: Impact of continental outflow during the late winter early spring, *J. Geophys. Res.*, 102, 28,469-28,487, 1997b.
- Crutzen, P. J., M. G. Lawrence, and U. Poschl, On the background photochemistry of tropospheric ozone, *Tellus*, 51, 123-146, 1999.
- Elliot S., D. R. Blake, R. A. Duce, C. A. Lai, I. McCreary, L. A. McNair, F. S. Rowland, A. G. Russell, G. E. Streit, and R. P. Turco, Motorization of China implies changes in Pacific air chemistry and primary production, *Geophys. Res. Lett.*, 24, 2671-2674, 1997.
- Guderian, R., D. T. Tingey, and R. Rabe, *Effects of photochemical oxidants on plants, in Air Pollution by Photochemical Oxidants: Formation, Transport, Control, and Effects on Plants*, R. Guderian (Ed.), p. 127-333, Springer-Verlag, Berlin, 1985.
- Guicherit, R., and M. Roemer, Tropospheric ozone trends, *Chemosphere*, 2, 167-183, 2000.
- Herring, J. A., D. A. Jaffe, H. J. Beine, S. Madronich, and D. R. Blake, High-latitude springtime photochemistry. Part II: Sensitivity studies of ozone production, *J. Atmos. Chem.*, 27, 155-178, 1997.
- Hauglustaine, D., S. Madronich, B. Ridley, J. Walega, C. Cantrell, R. Shetter, and G. Hübler, Observed and model-calculated photostationary state at Mauna Loa Observatory during MLOPEX 2, *J. Geophys. Res.*, 101, 14681-14696, 1996.
- Hauglustaine, D., S. Madronich, B. Ridley, S. J. Flocke, C. A. Cantrell, F. L. Eisele, R. E. Shetter, D. L. Tanner, P. Cinoux, and E. L. Atlas, Photochemistry and budget of ozone during the Mauna Loa observatory photochemistry experiment (MLOPEX2), *J. Geophys. Res.*, 104, 30275-30307, 1999.
- Horowitz, L. W., and D. J. Jacob, Global impacts of fossil fuel combustion on atmospheric NO_x, *J. Geophys. Res.*, 104, 23,823-23,840, 1999.
- Hov, O., F. Flatoy, T. Krognes, N. Schmidbauer, N. Heidam, O. Manscher, H. Lattila, H. Areskoug, M. Ferm, and A. Lindskog, The relationship between ozone, peroxyacetylnitrate and precursors in long range transport of photooxidants to Scandinavia, *Atmos. Environ.*, 31, 2853-2869, 1997.
- IPCC, Intergovernmental Panel on Climate Change, Contribution of Working Group I to the Second Assessment Report (J. T. Houghton, L. G. Meira Filho, B. A. Callander, N. Harris, A. Kattenberg, and K. Maskell, Eds.), *Climate Change 1995: The Science of Climate Change*, Cambridge Univ. Press, Cambridge, UK, 1996.
- Jacob D. J., B. G. Heikes, S. M. Fan, J. A. Logan, D. L. Mauzerall, J. D. Bradshaw, H. B. Singh, G. L. Gregory, R. W. Talbot, D. R. Blake, and G. W. Sachse, Origin of ozone and NO_x in the tropical troposphere: a photochemical analysis of aircraft observations over the South Atlantic basin, *J. Geophys. Res.*, 101, 24,235-24,250 1996.
- Jacob, D. J., J. A. Logan, and P. P. Murti, Effect of rising Asian emissions on surface ozone in the United States, *Geophys. Res. Lett.*, 26, 2175-2178, 1999.
- Jaeglé, L., D.J. Jacob, W. H. Brune, I. Faloon, D. Tan, B. G. Heikes, Y. Kondo, G. W. Sachse, B. Anderson, G. L. Gregory, H. B. Singh, R. Pueschel, G. Ferry, D. R. Blake, R. Shetter, Photochemistry of HO_x in the upper troposphere at northern midlatitudes, *J. Geophys. Res.*, 105, 3877-3892, 2000.

- Jaffe, D., T. Anderson, D. Covert, R. Kotchenruther, B. Trost, J. Danielson, W. Simpson, T. Berntsen, S. Karlsdottir, D. Blake, J. Harris, G. Carmichael, and I. Uno, Transport of Asian air pollution to North America, *Geophys. Res. Lett.*, 26, 711-714, 1999.
- Jaffe, D., T. Anderson, D. Covert, B. Trost, J. Danielson, W. Simpson, D. Blake, J. Harris, and D. Streets, Observations of ozone and related species in the northeast Pacific during the PHOBEA campaigns: 1. Ground based observations at Cheeka Peak, *J. Geophys. Res.*, 106, 7449-7461, 2001.
- Klonecki, A. and H. Levy, Tropospheric chemical ozone tendencies in CO-CH₄-NO_y-H₂O system: Their sensitivity to variations in environmental parameters and their application to a global chemistry transport model study, *J. Geophys. Res.*, 102, 21,221-21,237, 1997.
- Kotchenruther, R. A., D. A. Jaffe, H. J. Beine, T. L. Anderson, J. W. Bottenheim, J. M. Harris, D. R. Blake, and R. Schmitt, Observations of ozone and related species in the northeast Pacific during the PHOBEA campaigns: 2. Airborne observations, *J. Geophys. Res.*, 106, 7463-7483, 2001.
- Lacis A.A., D.J. Wuebbles, and J.A. Logan. Radiative forcing of global climate by changes in the vertical distribution of ozone. *J. Geophys. Res.*, 95, 9971-9981, 1990.
- Lee, S. H., H. Akimoto, H. Nakane, S. Kurnosenko, and Y. Kinjo, Lower tropospheric ozone trend observed in 1989-1997 at Okinawa, Japan, *Geophys. Res. Lett.*, 25, 1637-1640, 1998.
- Levy, H. Normal Atmosphere: Large Radical and Formaldehyde Concentrations Predicted. *Science* 173, 141-143, 1971.
- Logan, J. A., Trends in the vertical distribution of ozone: an analysis of ozonesonde data, *J. Geophys. Res.*, 99, 25,553-25,585, 1994.
- Mauzerall, D. L., D. Narita, H. Akimoto, L. Horowitz, S. Walters, D. A. Hauglustaine, and G. Brasseur, Seasonal characteristics of tropospheric ozone production and mixing ratios over East Asia: A global three-dimensional chemical transport model analysis, *J. Geophys. Res.*, 105, 17,895-17,910, 2000.
- McKeen, S., D. Kley, and A. Volz, *The historical trend of tropospheric ozone over western Europe: a model perspective*, in *Ozone in the Atmosphere*, R. D. Bojkov and P. Fabian, Eds., A. Deepak Publishing, Hampton, VA, 1989.
- Moxim W., H. Levy, and P. Kasibhatla, Simulated global tropospheric PAN: Its transport and impact on NO_x, *J. Geophys. Res.*, 101, 12621-12638, 1996.
- Schultz, M. G., D. J. Jacob, D. J. Bradshaw, S. T. Sandholm, J. E. Dibb, R. W. Talbot, and H. B. Singh, Chemical NO_x budget in the upper troposphere over the tropical South Pacific, *J. Geophys. Res.*, 105, 6669-6679, 2000.
- Singh, H. B., and L. J. Salas, Measurements of peroxyacetyl nitrate (PAN) and peroxypropionyl nitrate (PPN) at selected urban, rural and remote sites, *Atmos. Environ.*, 23, 231-238, 1989.
- Singh, H. B., D. Herlth, D. O'Hara, K. Zahnle, J. D. Bradshaw, S. T. Sandholm, R. Talbot, P. J. Crutzen, and M. Kanakidou, Relationship of peroxyacetyl nitrate to active and total odd nitrogen at northern high latitudes: influence of reservoir species on NO_x and O₃, *J. Geophys. Res.*, 97, 16,523-16,530, 1992.
- Streets D.G. and Waldhoff S.T. Present and future emissions of air pollutants in China: SO₂, NO_x, and CO. *Atm. Env.* 34, 363-374, 2000.
- Thakur, A. N., H. B. Singh, P. Mariani, Y. Chen, Y. Wang, D. J. Jacob, G. Brasseur, J. F. Muller, M. Lawrence, Distribution of reactive nitrogen species in the remote free troposphere: data and model comparisons, *Atmos. Environ.*, 33, 1403-1422, 1999.
- VanAardeen, J., G. Carmichael, H. Levy, D. Streets, and L. Hordijk, Anthropogenic NO_x emissions in Asia in the period 1990-2020, *Atmos. Environ.*, 33, 633-646, 1999.
- Volz, A. and D. Kley, Evaluation of the Montsouris series of ozone measurements made in the nineteenth century, *Nature*, 332, 240-242, 1988.
- Wang, Y. and D. Jacob, Anthropogenic forcing on tropospheric ozone and OH since preindustrial times, *J. Geophys. Res.*, 103, 31123-31135, 1998.
- Yienger, J. J., A. A. Klonecki, H. Levy, W. J. Moxim, and G. R. Carmichael, An evaluation of chemistry's role in the winter-spring ozone maximum found in the northern midlatitude free troposphere, *J. Geophys. Res.*, 104, 3655-3667, 1999.

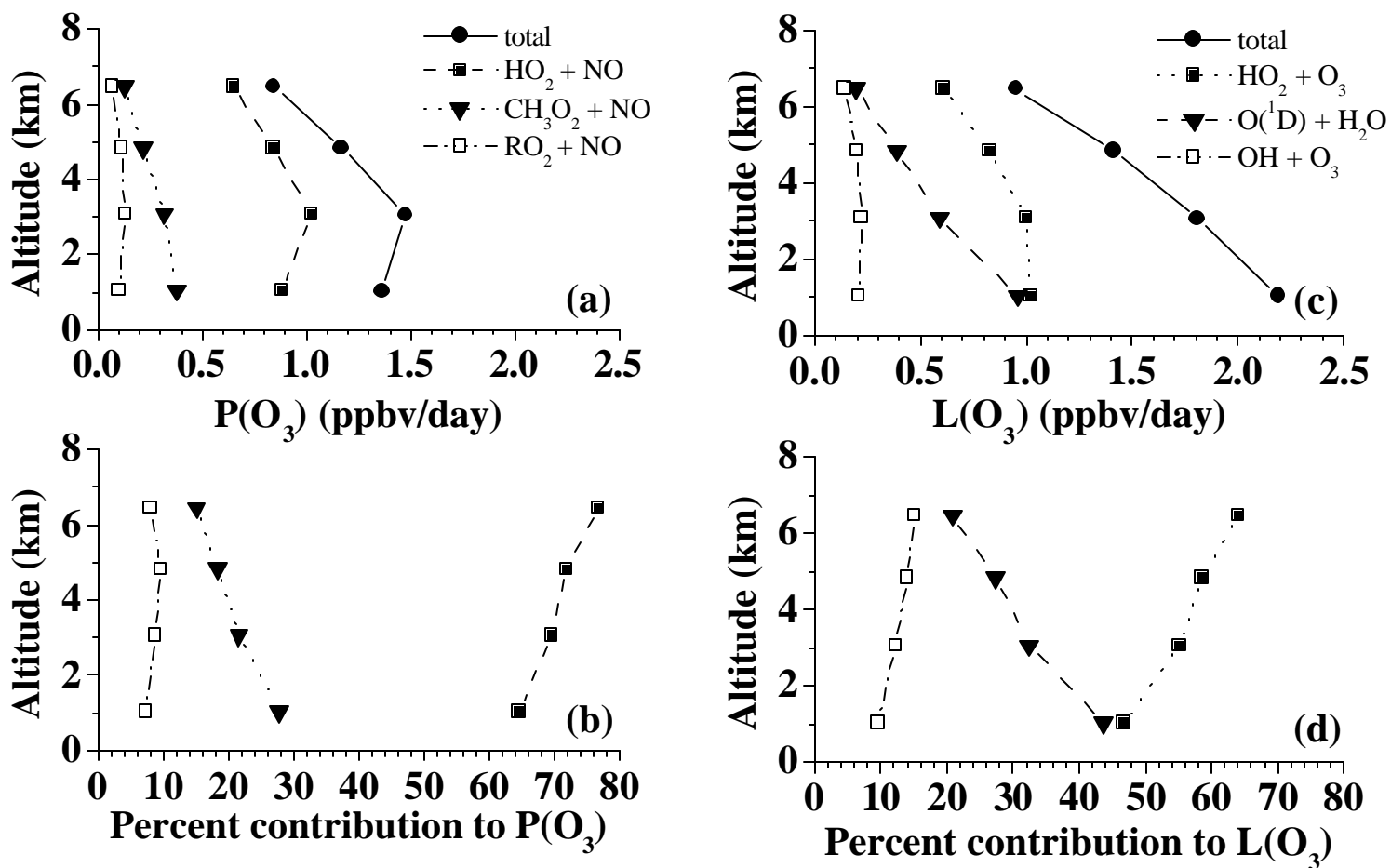


Figure 1. Ozone (a) production rates, $P(O_3)$, (b) the percent contribution to production, (c) loss rates, $L(O_3)$, and (d) the percent contribution to loss, delineated by reaction. All production and loss rates are averaged over the diel cycle.

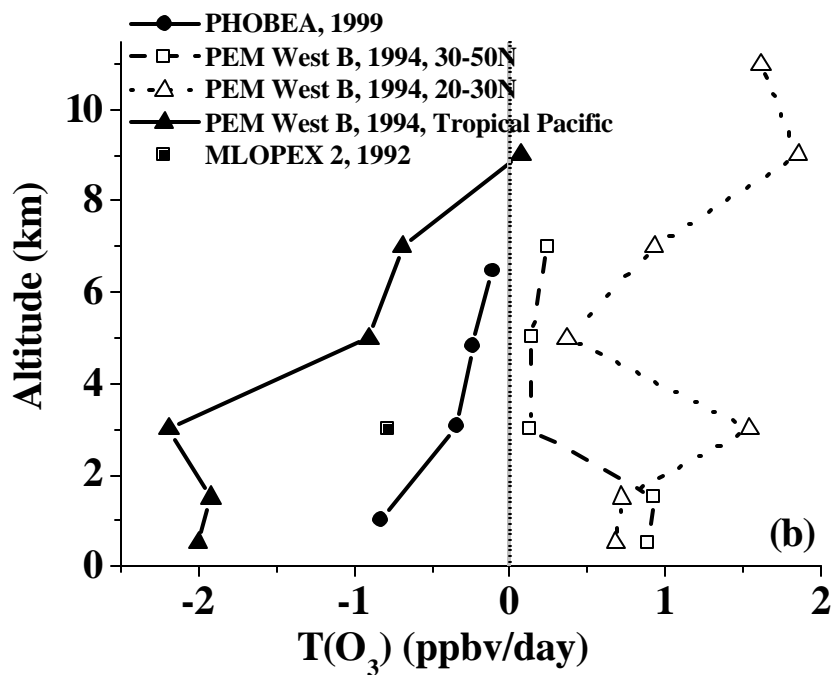
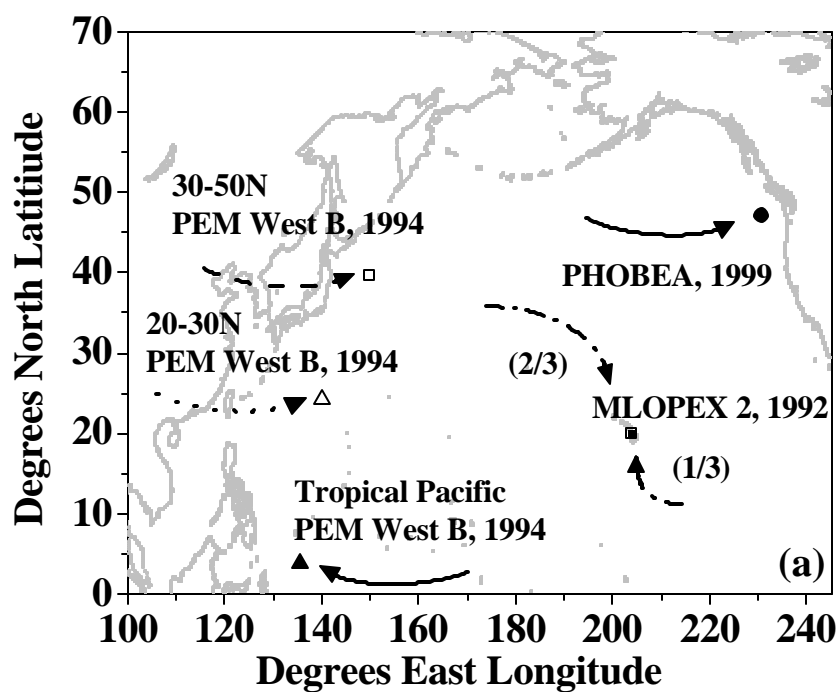


Figure 2. (a) Springtime North Pacific ozone photochemistry experiments in the 1990's. The dominant flow patterns during each experiment are indicated by arrows. (b) The springtime ozone photochemical tendency, $T(O_3)$, in the North Pacific as measured during the PHOBEA, PEM West B (Crawford et al., 1997a; Crawford et al., 1997b), and MLOPEX 2 (Hauglustaine et al., 1999) experiments. $T(O_3)$ is averaged over the diel cycle.

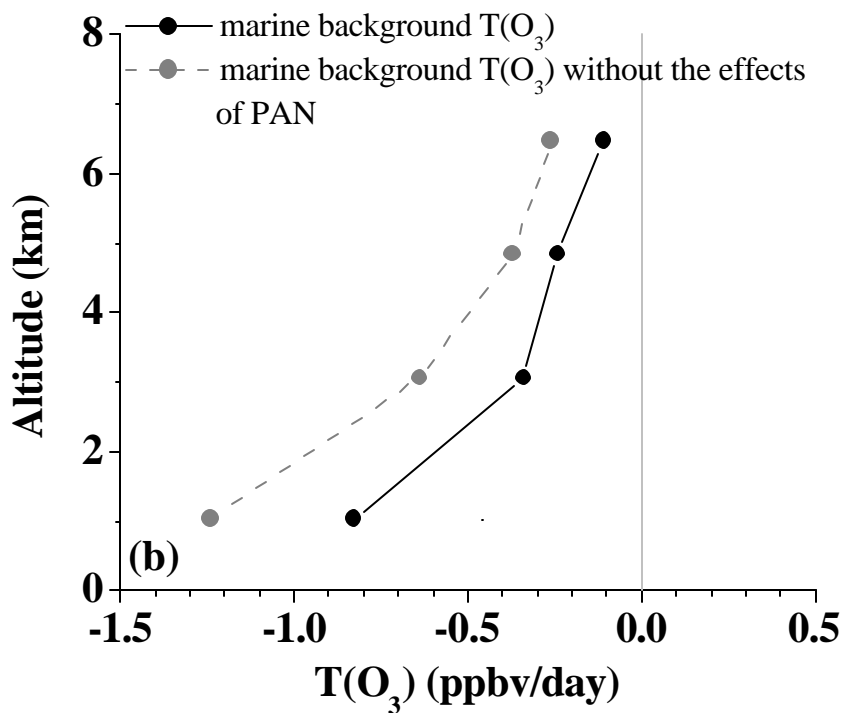
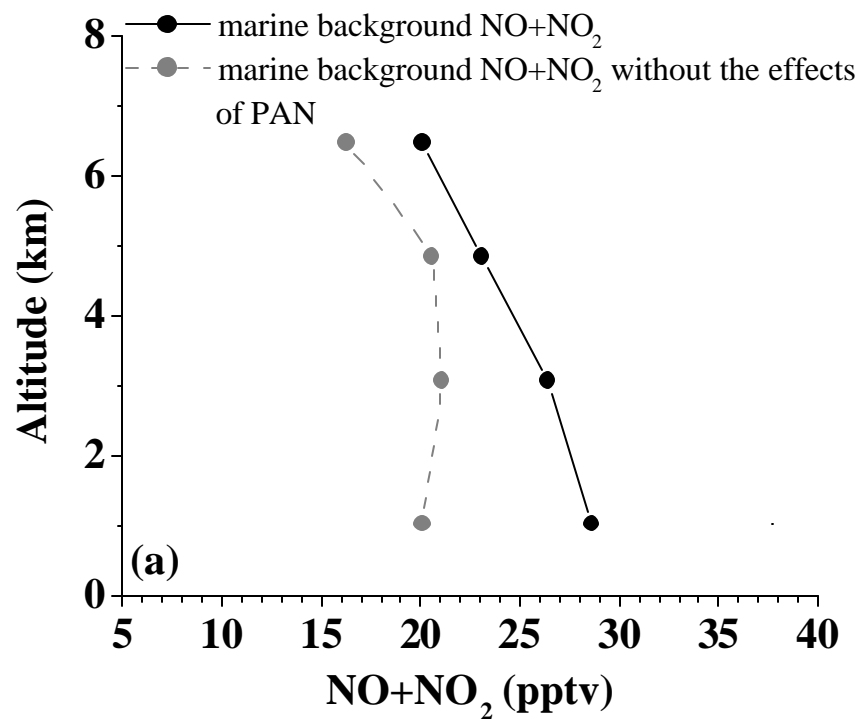


Figure 3. Model results for (a) NO+NO₂ near solar noon and (b) the ozone photochemical tendency, T(O₃), averaged over the diel cycle for the springtime Northeastern Pacific during the PHOBEA aircraft campaign. The marine background is presented as well as the effects of removing PAN decomposition from the marine background.

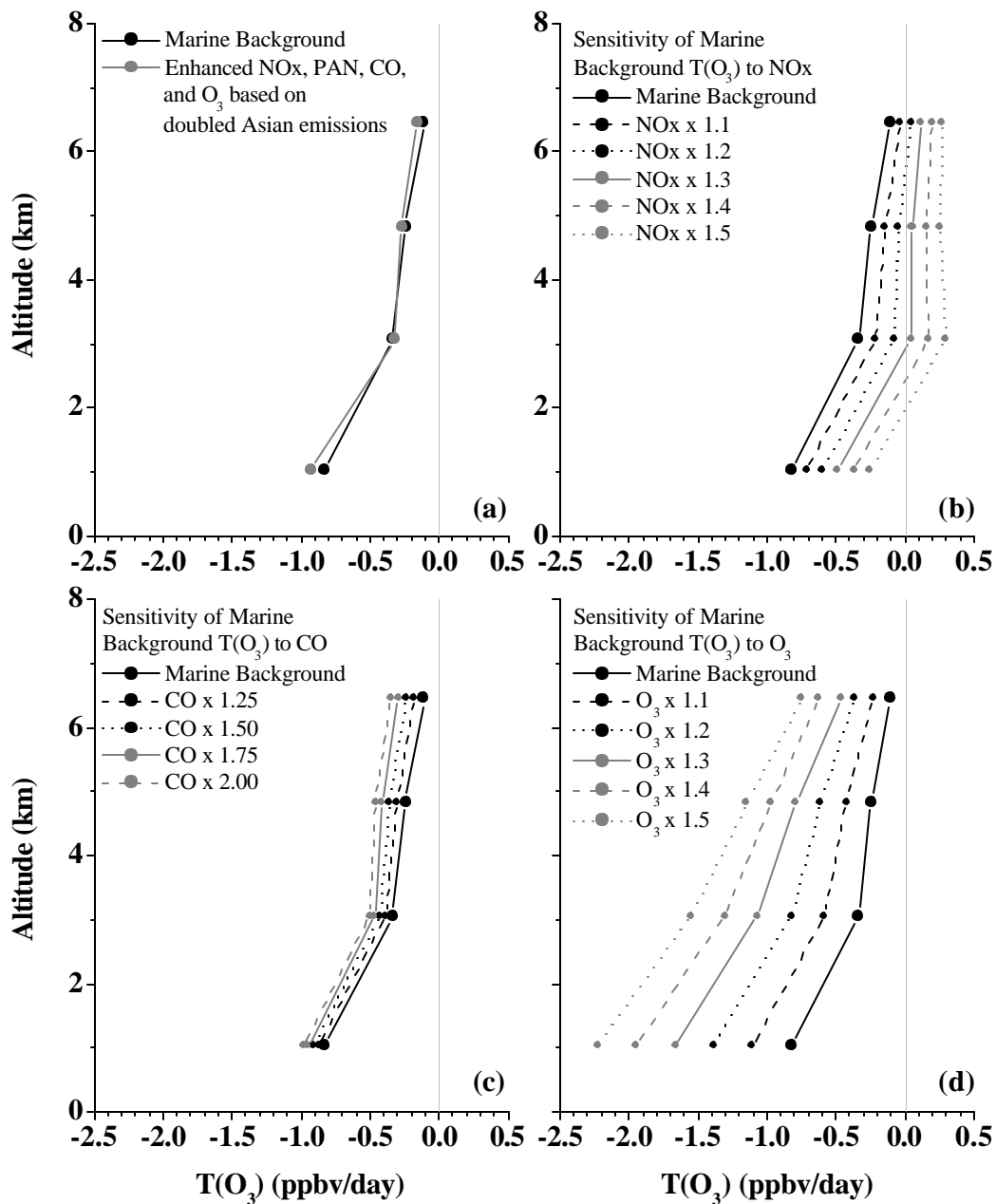


Figure 4. (a) The ozone photochemical tendency over the diel cycle, $T(O_3)$, of the marine background and after implementing enhanced NOx, PAN, CO, and O₃ in the Northeastern Pacific due to a doubling of Asian anthropogenic emissions, and sensitivity studies of $T(O_3)$ due to increasing (b) NOx, (c) CO, and (d) O₃, individually.

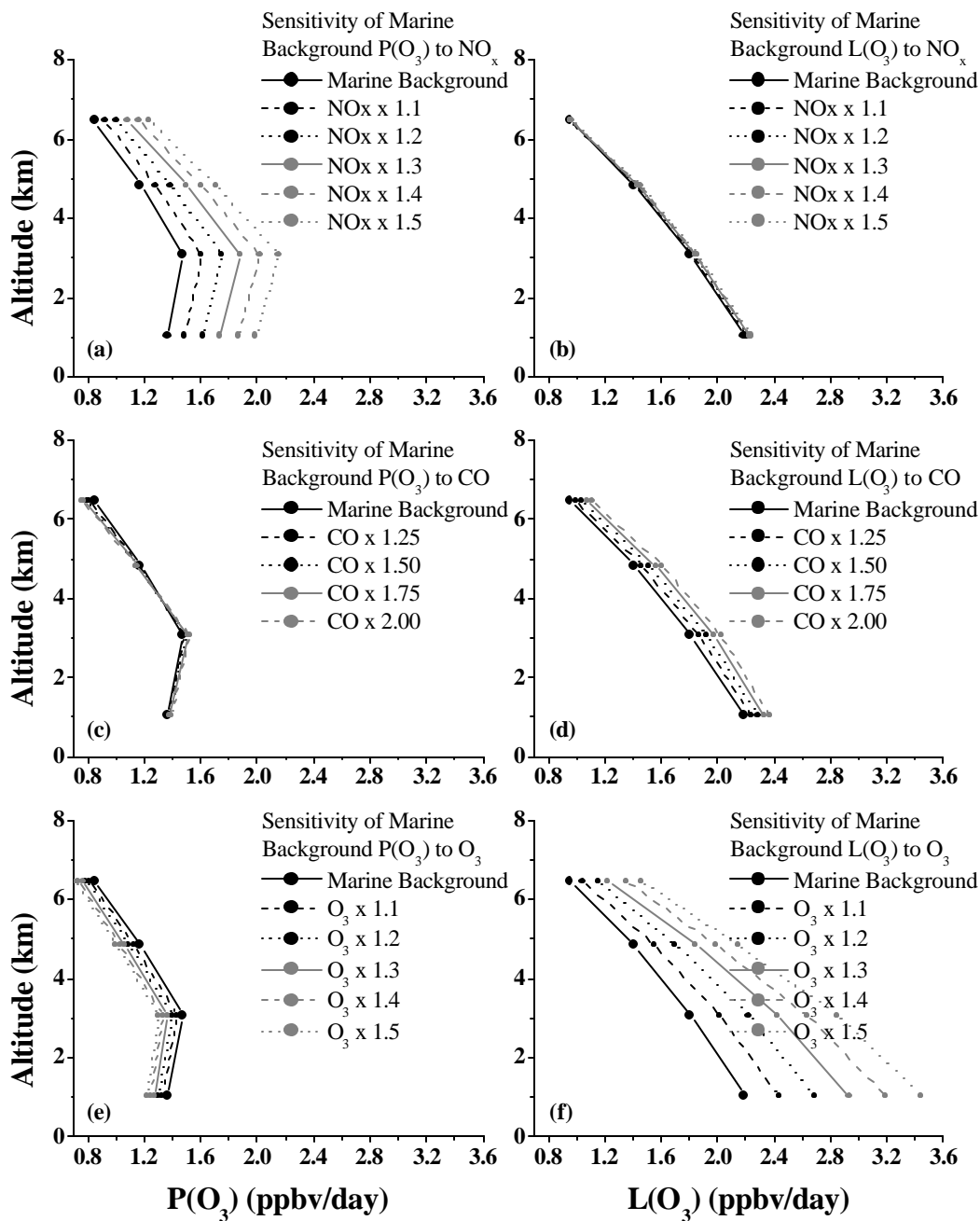


Figure 5. The sensitivity of $\text{P}(\text{O}_3)$ and $\text{L}(\text{O}_3)$ to increases in the marine background mixing ratios of NO_x (a,b), CO (c,d), and O_3 (e,f).

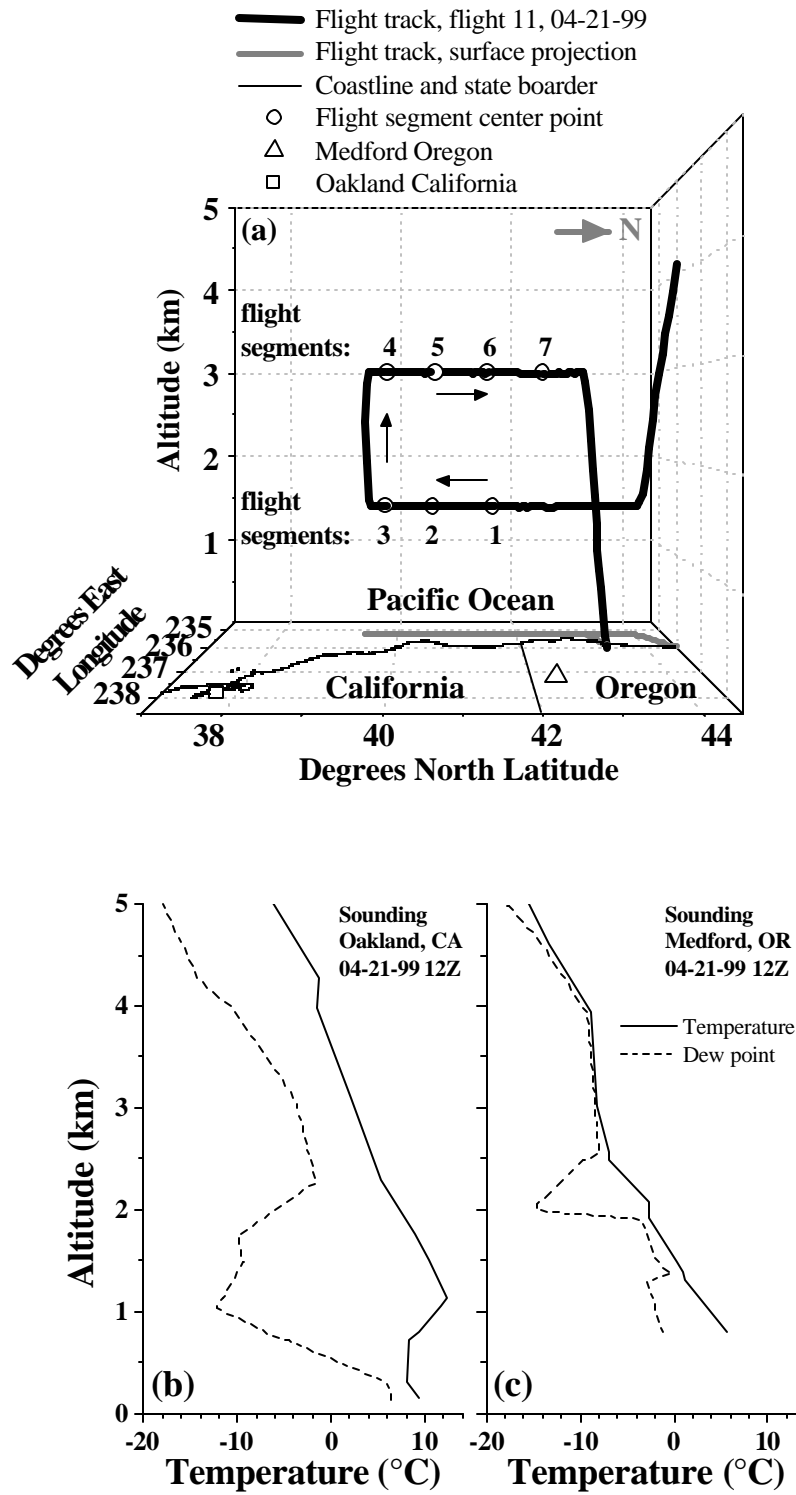


Figure 6. (a) Flight track for PHOBEA flight 11, April 21 1999, and 12Z data from atmospheric soundings at (b) Oakland California and (c) Medford Oregon.

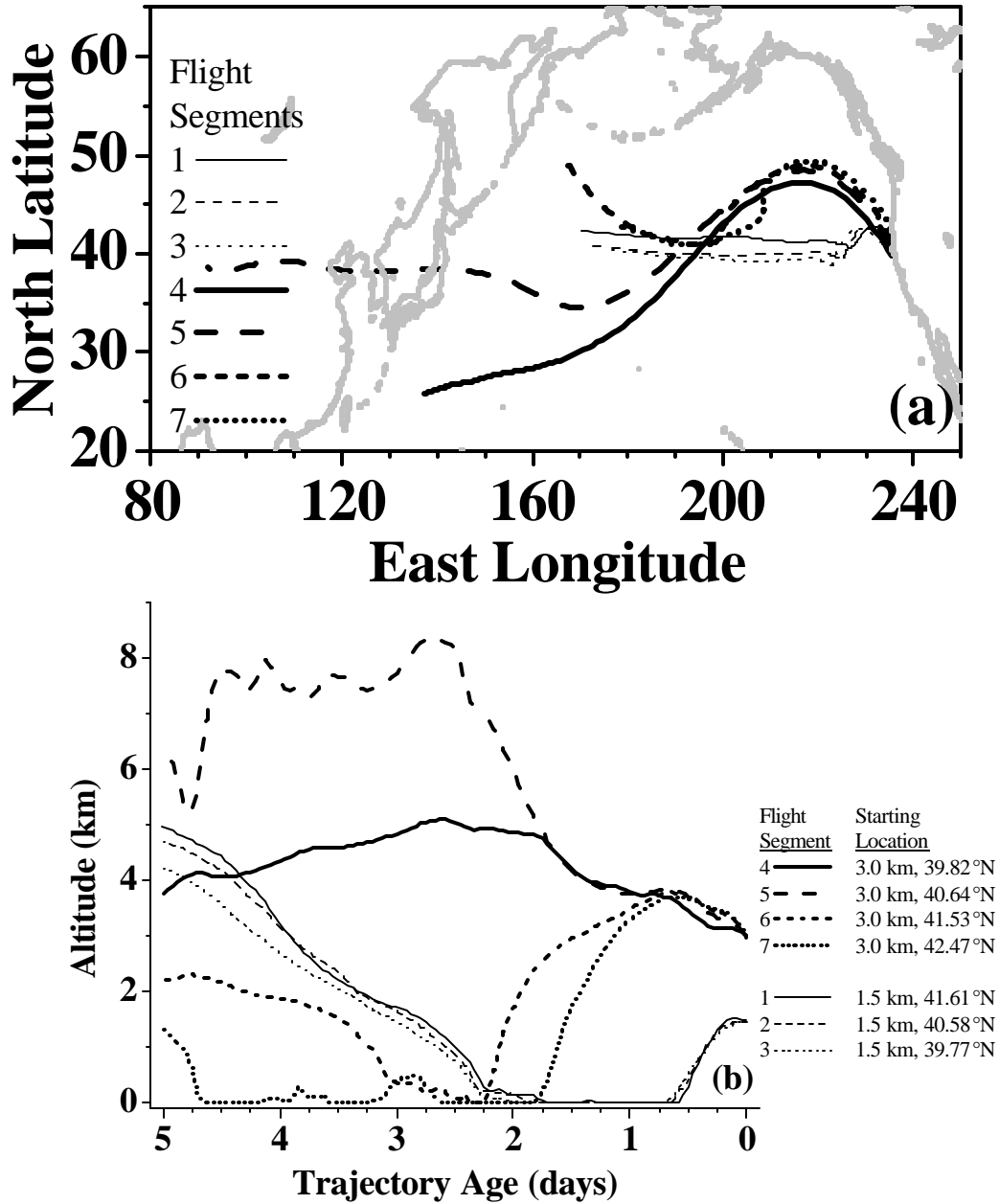


Figure 7. (a) Latitude longitude and (b) altitude age profiles for 5 day back isentropic trajectories during PHOBEA flight 11, April 21, 1999.

Table 1. Summary of PHOBEA observations (March 26 – April 28, 1999) used to constrain model calculations between 0 and 8 km altitude. Unless otherwise noted, chemical species are the average measured mixing ratios in pptv.

Observations	Layers (km)			
	0-2	2-4	4-6	6-8
pressure (mb)	895	692	546	436
temperature (K)	274.6	264.8	252.9	240.9
J(NO ₂) (s ⁻¹)	0.0093	0.0140	0.0147	0.0150
NO	9.5	12.5	12.5	12.9
PAN	78.5	183.0	206.2	185.8
PPN*	7.1	16.5	18.6	16.7
HNO ₃ †	132.1	139.8	146.7	156.6
O ₃ (ppbv)	47.4	59.5	71.7	79.3
H ₂ O (ppthv‡)	6.31	1.99	1.13	0.47
CO (ppbv)	138.6	138.9	132.2	130.1
methane (ppbv)	1830	1820	1800	1830
ethane	1580	1600	1580	1480
ethene	14.7	24.1	19.1	25.4
ethyne	365	406	392	337
propane	323	378	350	288
n-butane	72	91	85	60
i-butane	40	54	54	39
n-pentane	7.9	13.3	10.0	13.5
i-pentane	9.2	13.9	13.8	32.9
benzene	60	107	191	73
toluene	14	34	47	19
MeONO ₂	4.2	3.1	3.0	3.2
EtONO ₂	4.3	4.2	3.7	4.5
n-PrONO ₂	1.7	2.1	2.4	1.3
i-PrONO ₂	7.2	9.0	7.6	11.4
2-BuONO ₂	6.1	6.9	5.7	2.5

*PPN (peroxypropionyl nitrate) is specified based on a PPN/PAN ratio of 0.09 as per Singh and Salas (1989)

†HNO₃ is constrained based on previous measurements in this region as per Thakur et al. (1999), see text

‡parts per thousand by volume

Table 2. Selected mixing ratios (in pptv) and derived quantities from the 0-D model output. Unless otherwise noted, chemical species are the mixing ratios in pptv at the time of measurement (near solar noon), rates are averaged over the diel cycle.

Model Calculations	Layers (km)			
	0-2	2-4	4-6	6-8
NO _x *	31.4	33.4	45.6	64.2
NO ₂	19.3	14.1	10.5	7.3
HNO ₄	2.6	6.9	21.6	42.6
OH	0.13	0.16	0.16	0.14
OH (24 hour average)	0.04	0.05	0.05	0.05
HO ₂	16.2	17.0	14.9	12.2
HO ₂ (24 hour average)	5.9	6.2	5.6	4.9
CH ₃ O ₂	7.2	5.4	3.9	2.4
CH ₃ O ₂ (24 hour average)	3.3	2.6	2.0	1.4
NO _x production (pptv/day)	43.3	29.2	16.0	14.6
NO _x loss (pptv/day)	72.6	58.1	43.5	20.3
NO _x lifetime (days)†	0.43	0.57	1.05	3.16
O ₃ production; P(O ₃) (ppbv/day)	1.36	1.47	1.17	0.84
O ₃ loss; L(O ₃) (ppbv/day)	2.19	1.81	1.41	0.95
O ₃ tendency; T(O ₃) (ppbv/day)	-0.83	-0.34	-0.24	-0.11
PAN loss (pptv/day)	21.7	11.9	4.7	3.7
PAN's fractional contribution to NO _x	0.30	0.20	0.11	0.18
$\Delta P(O_3)_{PAN}$ (ppbv/day)‡	0.41	0.30	0.13	0.15

*NO_x is defined here as NO+NO₂+NO₃+2N₂O₅+HNO₂+HNO₄

†the lifetime of NO_x is defined as [NO_x]/(NO_x loss)

‡the enhancement in P(O₃) caused by PAN decomposition (equation 4, section 3.2)

Table 3. Selected measurements and model derived quantities for flight segments during PHOBEA flight 11, April 21, 1999.

Measured or Modeled Quantity	Flight Segments						
	1	2	3	4	5	6	7
Altitude (km)	1.5	1.5	1.5	3.0	3.0	3.0	3.0
Latitude (°N)	41.61	40.58	39.77	39.82	40.64	41.53	42.47
Temperature (°C)	2.2	4.4	5.5	1.9	1.2	-0.4	-2.3
Dew point temperature (°C)	2.0	3.9	4.8	-16.2	-17.2	-14.2	-13.1
NO (pptv)	8.9	5.0	7.1	14.9	10.6	4.8	4.3
PAN (pptv)	12.7	12.7	12.7	201.6	120.1	84.8	35.9
Ozone (ppbv)	44.5	35.8	49.4	78.7	70.8	51.1	49.8
H ₂ O (ppthv)	8.7	10.3	11.1	2.1	2.0	2.5	2.8
NO _x (pptv)*	27.4	13.6	21.7	40.1	28.1	10.7	9.7
NO _x loss (pptv/day)	91.4	50.8	105.6	148.4	91.6	33.8	28.2
O ₃ production; P(O ₃) (ppbv/day)	1.76	1.09	1.87	2.89	1.84	0.87	0.76
O ₃ loss; L(O ₃) (ppbv/day)	3.59	3.51	6.09	4.67	3.50	2.74	2.59
O ₃ tendency; T(O ₃) (ppbv/day)	-1.83	-2.42	-4.22	-1.78	-1.66	-1.87	-1.83
PAN loss (pptv/day)	4.6	8.1	9.1	74.4	41.2	28.5	8.6
PAN's fractional contribution to NO _x	0.05	0.16	0.09	0.50	0.45	0.84	0.30
$\Delta P(O_3)_{PAN}$ (ppbv/day)†	0.09	0.17	0.17	1.45	0.83	0.73	0.23

*NO_x is defined here as NO+NO₂+NO₃+2N₂O₅+HNO₂+HNO₄

†the enhancement in P(O₃) caused by PAN decomposition (equation 4, section 3.2)